Journal of Polymer Science and Engineering 2024, 7(1), 5170.
https://doi.org/10.24294/jpse.v7i1.5170

Article

Mechanical strength investigation of chemically reinforced sandy soil using organic copolymers for geotechnical engineering applications

Mohan Raj Krishnan*, **Edreese Housni Alsharaeh***

College of Science and General Studies, AlFaisal University, P.O. Box 50927, Riyadh 11533, Saudi Arabia
* **Corresponding authors:** Mohan Raj Krishnan, mkrishnan@alfaisal.edu; Edreese Housni Alsharaeh, ealsharaeh@alfaisal.edu

CITATION

Krishnan MR, Alsharaeh EH. Mechanical strength investigation of chemically reinforced sandy soil using organic copolymers for geotechnical engineering applications. Journal of Polymer Science and Engineering. 2024; 7(1): 5170. https://doi.org/10.24294/jpse.v7i1.5170

ARTICLE INFO

Received: 12 March 2024
Accepted: 6 May 2024
Available online: 16 May 2024

Abstract: The chemical reinforcement of sandy soils is usually carried out to improve their properties and meet specific engineering requirements. Nevertheless, conventional reinforcement agents are often expensive; the process is energy-intensive and causes serious environmental issues. Therefore, developing a cost-effective, room-temperature-based method that uses recyclable chemicals is necessary. In the current study, poly (styrene-co-methyl methacrylate) (PS-PMMA) is used as a stabilizer to reinforce sandy soil. The copolymer-reinforced sand samples were prepared using the one-step bulk polymerization method at room temperature. The mechanical strength of the copolymer-reinforced sand samples depends on the ratio of the PS-PMMA copolymer to the sand. The higher the copolymer-to-sand ratio, the higher the sample's compressive strength. The sand (70 wt.%)-PS-PMMA (30 wt.%) sample exhibited the highest compressive strength of 1900 psi. The copolymer matrix enwraps the sand particles to form a stable structure with high compressive strengths.

Keywords: sand; copolymer; polystyrene; polymethyl methacrylate; soil reinforcement; geotechnical

1. Introduction

Natural sandy soils are unsuitable for geotechnical engineering applications due to their low strength, loose structure, and high saturated liquefaction potential [1–3]. Therefore, chemical reinforcement of sandy soil is widely employed in geotechnical engineering [4]. The traditional sand reinforcement agents are lime [5], fly ash [6], gypsum [7], cement [8], zeolite [9–11], etc. Though these reinforcement agents for improvement have apparent advantages, the modifications made using these chemical additives often increase the modified sand's pH value and cause groundwater pollution and other environmental issues [4]. To overcome these potential limitations of conventional soil reinforcement agents, non-conventional chemical additives such as polymers [12], resins [13], enzymes [14], ions [15], and lignin derivatives [16]-based reinforcement agents are developed to meet the physical and engineering requirements of the sandy soil for different engineering purposes [17].

Various polymer systems have been systematically studied for successful sand reinforcements [18,19]. Polymer and polymer nanocomposite materials are found to be potential candidates for improving the compressibility strength of sandy soil [20] and various other applications [21–43]. Also, the polymer materials can enwrap the sand particles and improve their strength by filling the void spaces between them [44]. Krishnan et al. recently reported a series of research works to improve the crush resistance of sand particles by dual polymer nanocomposite coating onto the sand surfaces [45–49]. Krishnan et al. also reported sand particle modifications with polyacrylamide (PAM) gels at elevated temperatures for petroleum and natural gas engineering applications [50–56]. The same group reported various significant works of different industrial importance processes based on polymer composite systems [51,54,57–60]. The PAM-modified sand particles are also used for agricultural purposes in deserts [45,60]. Xanthum gum, an eco-friendly organic polymer, was also studied for coastal agriculture, reducing coastal erosion issues. Naeini et al. studied the mechanical strength improvement of sand particles by epoxy resin modification. It was also found that the modification of epoxy resin in sand particles enhanced elastic modulus under wet and dry conditions. Yang et al. reported polyaspartic acid resin as a novel sand-fixing agent. As evident from the recent research reports, polymeric materials can act as a potential reinforcement agent for sandy soil.

The current work aims to study the effect of PS-PMMA copolymer as a chemical reinforcing agent for sandy soil. The compressibility strengths of the PS-PMMA copolymer-reinforced sand samples were evaluated. Different concentrations of PS-PMMA copolymer and sand were chosen to determine the effect of the copolymer on the sand's compressibility and strength enhancement. The results and associated discussion provide information on the chemical stabilization mechanisms of polymer-reinforced sand for researchers and practicing engineers.

2. Experimental

2.1. Materials

Styrene (S; >99% purity) was purchased from Sigma Aldrich. Methylmethacrylate (MMA; 99% purity) was purchased from Aldrich. Benzoyl peroxide (BPO; >90% purity) was purchased from Loba Chemie. Dimethyl-p-toluidine (DMPT; >99% purity) was purchased from Alfa Aser. All the chemicals are of analytical grade and used as received. Sandy soil samples (70/40 mesh) were collected from the Saudi Desert.

2.2. Methods

2.2.1. Preparation of PS-PMMA reinforced sandy soil

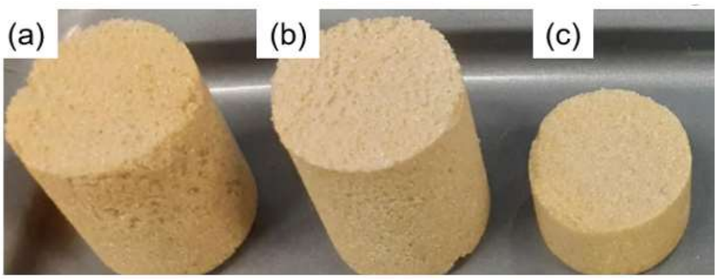

Figure 1. Cylindrical blocks of PS-PMMA reinforced sandy soils of different heights. **(a)** 10 cm; **(b)** 7 cm; and **(c)** 3 cm.

To prepare PS-PMMA-reinforced sandy soil, the sand particles were well mixed to a 30 wt.% of a 1:1 wt.% co-monomer mixture of S and MMA along with BPO (0.01 wt.% related to the monomers) and 0.001 wt.% of DMPT at room temperature. The mixed sand samples were aged 10–15 min for the completion of the polymerization reaction. The sand samples were prepared in a cylindrical glass tube to prepare the cylindrical-shaped samples (**Figure 1**). After the sand samples were hardened, the glass tubes were broken to retrieve the sand samples.

2.2.2. Calculation of bulk volume, grain volume, and pore volume

The samples' bulk volume (cc), pore volume, and grain volumes are calculated using Equations (1)–(3).

$$Bulk\ volume\ of\ the\ cylindrical\ sample = \pi r^2 h \tag{1}$$

'h' is the height of the cylindrical sample.

The samples' pore volumes (cc) were determined by the liquid saturation method. The samples are initially immersed in methanol, and after 60 min, the excess methanol is decanted, and the sample is weighed again. The pore volume of the sample is calculated using the initial and liquid pore-filled sample weights (Equation (2)).

$$The\ pore\ volume\ of\ the\ sample = \frac{Weight\ of\ the\ MeOH\ saturated\ sample - Weight\ of\ the\ dried\ sample}{Density\ of\ MeOH} \tag{2}$$

$$Grain\ Volume = Bulk\ Volume - Pore\ volume \tag{3}$$

2.2.3. Compressibility tests

Figure 2. Compressibility test of the copolymer-reinforced cylindrical sand blocks. The inset shows the cracked block after the block is compressed.

The compressibility test has been carried out using a Specac mechanical compressor (**Figure 2**). The cylindrical sample block is placed on a supporting bottom, and specific pressure is applied through a circular pressure head. The pressure rises and suddenly drops when the block starts cracking (**Figure 2**). The maximum pressure the sample block tolerated before cracking down is calculated as its compressibility strength (Equation (4)).

$$Pressure = Force/Area \quad (4)$$

3. Results and discussion

3.1. PS-PMMA copolymer reinforced sand blocks

The stepwise preparation of PS-PMMA copolymer-reinforced sand blocks at room temperature is schematically illustrated in **Figure 3**. The sand particles were mixed with the required amount of a co-monomer mixture of S, MMA, BPO, and DMPT to prepare the samples. This subsequently allowed for random copolymerization at room temperature. The BPO undergoes decomposition in the presence of DMPT and produces BPO free radicals. The co-monomer molecules were synchronously transformed into co-monomer free radicals with the aid of the BPO initiator radicals. After that, the co-monomer free radicals became radical donors to the neighboring co-monomer molecules. Consequently, a chain propagation of S and MMA monomers took place, which resulted in the growth of PS-PMMA random copolymer chain radicals [61,62]. Finally, the copolymer chain radicals were terminated either by dimerization or disproportionation. The formed PS-PMMA copolymer on sand surfaces efficiently wraps the sand particles.

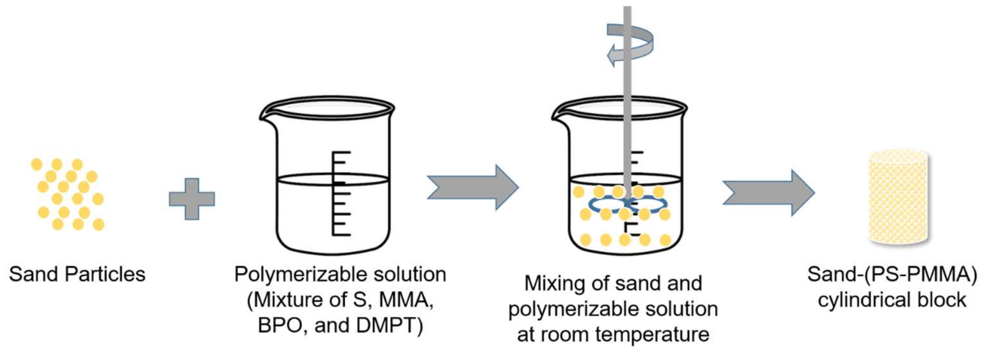

Figure 3. Schematic illustration of the preparation of PS-PMMA copolymer reinforced sand (sand-(PS-PMMA) cylindrical block).

3.2. Bulk, grain, and pore volumes of PS-PMMA copolymer-reinforced sand

Photographs of PS-PMMA copolymer-reinforced sand samples are shown in **Figure 4**. As evident from **Figure 4a–c**, when the copolymer concentration is low relative to sand (i.e., 1 wt.%, 5 wt.%, and 10 wt.%), the sand particles either remain free or agglomerated, while if the concentration is increased to 15 wt.% and above (20 wt.% and 30 wt.%), sand-polymer blocks are obtained. When the PS-PMMA concentration is increased beyond 30 wt.% to sand, the sand particles are well-buried into the polymer matrix, which is no longer a homogenous composite of sand-PS-PMMA copolymer. The shape of the blocks can be manipulated using respective shaped templates. In this study, we prepared the samples in cylindrical geometries to evaluate the bulk, grain, and pore volumes and the effect of PS-PMMA copolymer concentration on these structural parameters (**Figure 5**). In the sample with 15 wt.% of PS-PMMA, the bulk, grain, and pore volumes are 50 cc, 32 cc, and 18 cc, respectively. At the same time, for the sample with 20 wt.% PS-PMMA, the bulk, grain, and pore volumes are 50 cc, 40.8 cc, and 9.2 cc, respectively, while for the sample with 30 wt.% PS-PMMA, the bulk, grain, and pore volumes are 50 cc, 46.1 cc, and 3.9 cc, respectively. The geometric and pore characteristics of the samples are summarized in **Table 1**. For the fixed bulk volume of the copolymer-reinforced sand blocks, with an increase in the polymer concentration, the porosity decreases while the grain volume increases. The samples' increased grain and decreased pore volumes are attributed to the successful coating of the copolymer onto the sand particles while efficiently wrapping them.

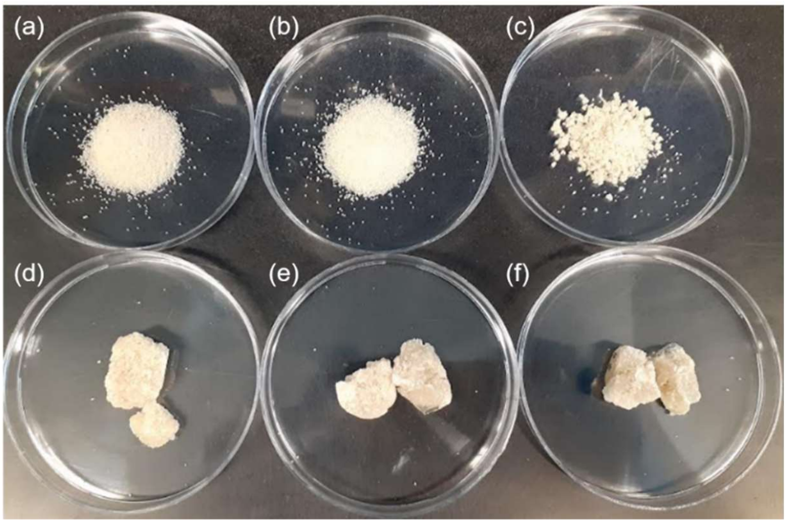

Figure 4. Photographs of Sand-Copolymer samples prepared at room temperature. **(a)** Sand (99%)-(PS-PMMA)(1%); **(b)** Sand (95%)-(PS-PMMA)(5%); **(c)** Sand (90%)-(PS-PMMA)(10%); **(d)** Sand (85%)-(PS-PMMA)(15%); **(e)** Sand (80%)-(PS-PMMA)(20%); **(f)** Sand (70%)-(PS-PMMA)(30%).

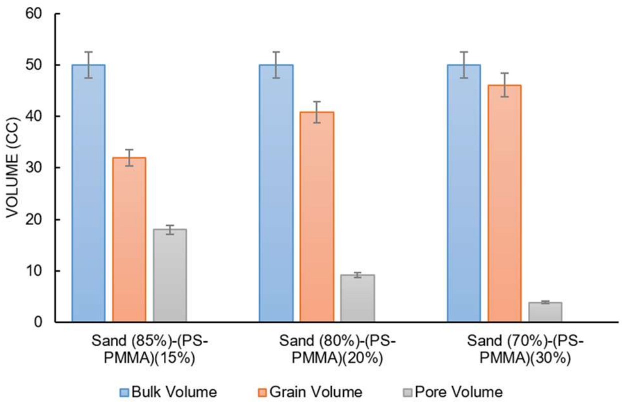

Figure 5. Bulk, grain, pore volumes, and porosity of sand (85%)-(PS-PMMA)(15%), sand (80%)-(PS-PMMA)(20%), and sand (70%)-(PS-PMMA)(30%) samples.

The calculated geometric and pore characteristics of the PS-PMMA copolymer-reinforced sand samples are summarized in **Table 1**.

Table 1. Geometric and pore characteristics of the PS-PMMA copolymer-reinforced sand samples.

S.No.	Sample	Bulk volume (cc)	Grain volume (cc)	Pore volume (cc)
1.	Sand (99%)-(PS-PMMA)(1%)	Individual Grains	Individual Grains	-
2.	Sand (95%)-(PS-PMMA)(5%)	Individual Grains	Individual Grains	-
3.	Sand (90%)-(PS-PMMA)(10%)	Agglomerated Grains	Agglomerated Grains	-
4.	Sand (85%)-(PS-PMMA)(15%)	50	32	18
5.	Sand (80%)-(PS-PMMA)(20%)	50	40.8	9.2
6.	Sand (70%)-(PS-PMMA)(30%)	50	46.1	3.9

3.3. Compressibility strength of PS-PMMA copolymer-reinforced sand

Figure 6 shows the compressibility strengths of the PS-PMMA copolymer-reinforced samples—the compressibility strengths for the sand samples with 1 wt.%, 5 wt.%, and 10 wt.% PS-PMMA copolymers were not determined as they are either free or agglomerated particles. The compressibility strengths of sand (85%)-(PS-PMMA)(15%), sand (80%)-(PS-PMMA)(20%), and sand (70%)-(PS-PMMA)(30%) are evaluated to be 224 psi, 1500 psi, and 1900 psi. The compressibility strengths of PS-PMMA copolymer-reinforced sand samples are summarized in **Table 2**. If the copolymer concentration of the reinforced sand samples was high, the compressibility strengths were also found to be high [63]. This increase in the samples' mechanical strength is attributed to the addition of high-strength thermoplastic polymers to the sand and the successful cross-linking of copolymers with the sand surfaces [30,31,33,34,40,45–50,55,56,60].

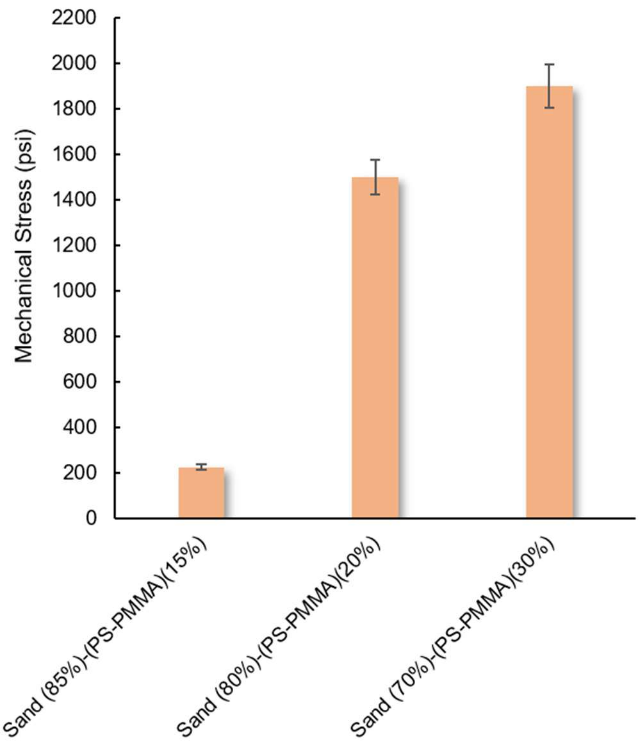

Figure 6. Compressibility strength of sand (85%)-(PS-PMMA)(15%), sand (80%)-(PS-PMMA)(20%), and sand (70%)-(PS-PMMA)(30%) samples.

Table 2. Compressibility strengths of the PS-PMMA copolymer-reinforced sand samples.

S.No.	Sample	The shape of the sample	Compressibility strength (psi)
1.	Sand (99%)-(PS-PMMA)(1%)	Individual Grains	-
2.	Sand (95%)-(PS-PMMA)(5%)	Individual Grains	-
3.	Sand (90%)-(PS-PMMA)(10%)	Agglomerated Grains	-
4.	Sand (85%)-(PS-PMMA)(15%)	Cylindrical	224
5.	Sand (80%)-(PS-PMMA)(20%)	Cylindrical	1500
6.	Sand (70%)-(PS-PMMA)(30%)	Cylindrical	1900

4. Conclusion

The current work reports a cost-effective preparation method of mechanically reinforced sand particles using PS-PMMA copolymer. A one-step bulk polymerization technique was used to coat the sand particles with the PS-PMMA copolymer. When the BPO is in contact with DMPT at room temperature, the BPO instantaneously decomposes to form free radicals. The free radicals react with the monomers and form co-monomer free radicals. The co-monomer free radicals randomly react to form the co-polymer onto the sand particles. The compressibility strength of the copolymer-reinforced sand blocks is directly proportional to the sand-to-copolymer ratio. The higher the sand-to-copolymer ratio, the higher the strength of the sand block. Simultaneously, the porosity is inversely related to the sand-to-copolymer ratio. The sand (70 wt.%)-PS-PMMA (30 wt.%) sample exhibited a high compressive strength of 1900 psi. The copolymer matrix enwraps the sand particles to form a stable structure with high compressive strengths.

Author contributions: Experimental studies, MRK; data analyses, MRK and EHA; original manuscript writing, MRK and EHA; supervised the project, EHA. All authors have read and agreed to the published version of the manuscript.

Data availability statement: The data will be available based on a request from the corresponding author.

Funding: This research was funded by Alfaisal University grant number 726174. The authors gratefully acknowledge Alfaisal University and its Office of Research & Innovation for their continuous support throughout this study.

Conflict of interest: The authors declare no conflict of interest.

References

1. Bao X, Jin Z, Cui H, et al. Soil liquefaction mitigation in geotechnical engineering: An overview of recently developed methods. Soil Dynamics and Earthquake Engineering. 2019; 120: 273-291. doi: 10.1016/j.soildyn.2019.01.020
2. Liu L, Cai G, Zhang J, et al. Evaluation of engineering properties and environmental effect of recycled waste tire-sand/soil in geotechnical engineering: A compressive review. Renewable and Sustainable Energy Reviews. 2020; 126: 109831. doi: 10.1016/j.rser.2020.109831
3. Ostovar M, Ghiassi R, Mehdizadeh MJ, et al. Effects of Crude Oil on Geotechnical Specification of Sandy Soils. Soil and Sediment Contamination: An International Journal. 2020; 30(1): 58-73. doi: 10.1080/15320383.2020.1792410
4. Wei X, Ku T. New design chart for geotechnical ground improvement: characterizing cement-stabilized sand. Acta Geotechnica. 2019; 15(4): 999-1011. doi: 10.1007/s11440-019-00838-2

5. Abbasi N, Mahdieh M. Improvement of geotechnical properties of silty sand soils using natural pozzolan and lime. International Journal of Geo-Engineering. 2018; 9(1): 1–12.
6. Simatupang M, Mangalla LK, Edwin RS, et al. The Mechanical Properties of Fly-Ash-Stabilized Sands. Geosciences. 2020; 10(4): 132. doi: 10.3390/geosciences10040132
7. Pu S, Zhu Z, Huo W. Evaluation of engineering properties and environmental effect of recycled gypsum stabilized soil in geotechnical engineering: A comprehensive review. Resources, Conservation and Recycling. 2021; 174: 105780. doi: 10.1016/j.resconrec.2021.105780
8. Fabiano E, Reginaldo SP, Eder PM, et al. Improving geotechnical properties of a sand-clay soil by cement stabilization for base course in forest roads. African Journal of Agricultural Research. 2017; 12(30): 2475-2481. doi: 10.5897/ajar2016.12482
9. Jafarpour P, Ziaie Moayed R, Kordnaeij A. Yield stress for zeolite-cement grouted sand. Construction and Building Materials. 2020; 247: 118639. doi: 10.1016/j.conbuildmat.2020.118639
10. Mola-Abasi H, Kordtabar B, Kordnaeij A. Effect of Natural Zeolite and Cement Additive on the Strength of Sand. Geotechnical and Geological Engineering. 2016; 34(5): 1539-1551. doi: 10.1007/s10706-016-0060-4
11. ShahriarKian M, Kabiri S, Bayat M. Utilization of Zeolite to Improve the Behavior of Cement-Stabilized Soil. International Journal of Geosynthetics and Ground Engineering. 2021; 7(2). doi: 10.1007/s40891-021-00284-9
12. Fatehi H, Ong DEL, Yu J, et al. Biopolymers as Green Binders for Soil Improvement in Geotechnical Applications: A Review. Geosciences. 2021; 11(7): 291. doi: 10.3390/geosciences11070291
13. Anagnostopoulos CA, Kandiliotis P, Lola M, et al. Improving Properties of Sand Using Epoxy Resin and Electrokinetics. Geotechnical and Geological Engineering. 2014; 32(4): 859-872. doi: 10.1007/s10706-014-9763-6
14. Ahenkorah I, Rahman MM, Karim MR, et al. A comparison of mechanical responses for microbial- and enzyme-induced cemented sand. Géotechnique Letters. 2020; 10(4): 559-567. doi: 10.1680/jgele.20.00061
15. Refaei M, Arab MG, Omar M. Sandy Soil Improvement through Biopolymer Assisted EICP. Geo-Congress 2020. Published online February 21, 2020. doi: 10.1061/9780784482780.060
16. Lin G, Liu W, Zhao J, et al. Experimental investigation into effects of lignin on sandy loess. Soils and Foundations. 2023; 63(5): 101359. doi: 10.1016/j.sandf.2023.101359
17. Chang I, Lee M, Tran ATP, et al. Review on biopolymer-based soil treatment (BPST) technology in geotechnical engineering practices. Transportation Geotechnics. 2020; 24: 100385. doi: 10.1016/j.trgeo.2020.100385
18. Al-Khanbashi A, Abdalla SW. Evaluation of three waterborne polymers as stabilizers for sandy soil. Geotechnical and Geological Engineering. 2006; 24(6): 1603-1625. doi: 10.1007/s10706-005-4895-3
19. Liu J, Bai Y, Song Z, et al. Stabilization of sand using different types of short fibers and organic polymer. Construction and Building Materials. 2020; 253: 119164. doi: 10.1016/j.conbuildmat.2020.119164
20. Sarkar D, Lieske W, Goudarzy M, et al. The influence of polymer content on the shear wave velocities in fine sand. Environmental Geotechnics. 2024; 11(2): 64-64. doi:10.1680/jenge.23.00017
21. Aldosari MA, Alsaud KBB, Othman A, et al. Microwave Irradiation Synthesis and Characterization of Reduced-(Graphene Oxide-(Polystyrene-Polymethyl Methacrylate))/Silver Nanoparticle Nanocomposites and Their Anti-Microbial Activity. Polymers. 2020; 12(5): 1155. doi: 10.3390/polym12051155
22. Almohsin A, Michal F, Alsharaeh E, et al. Self-Healing PAM Composite Hydrogel for Water Shutoff at High Temperatures: Thermal and Rheological Investigations. Day 2 Tue, October 22, 2019. Published online October 21, 2019. doi: 10.2118/198664-ms
23. Bongu CS, Krishnan MR, Soliman A, et al. Flexible and Freestanding MoS2/Graphene Composite for High-Performance Supercapacitors. ACS Omega. 2023; 8(40): 36789-36800. doi: 10.1021/acsomega.3c03370
24. Cheng CF, Chen YM, Zou F, et al. Li-Ion Capacitor Integrated with Nano-network-Structured Ni/NiO/C Anode and Nitrogen-Doped Carbonized Metal–Organic Framework Cathode with High Power and Long Cyclability. ACS Applied Materials & Interfaces. 2019; 11(34): 30694-30702. doi: 10.1021/acsami.9b06354
25. Chien YC, Huang LY, Yang KC, et al. Fabrication of metallic nanonetworks via templated electroless plating as hydrogenation catalyst. Emergent Materials. 2020; 4(2): 493-501. doi: 10.1007/s42247-020-00108-y
26. Keishnan MR, Michael FM, Almohsin AM, et al. Thermal and Rheological Investigations on N,N'-Methylenebis Acrylamide Cross-Linked Polyacrylamide Nanocomposite Hydrogels for Water Shutoff Applications. Day 4 Thu, November 05, 2020. Published online October 27, 2020. doi: 10.4043/30123-ms

27. Krishnan M, Michal F, Alsoughayer S, et al. Thermodynamic and Kinetic Investigation of Water Absorption by PAM Composite Hydrogel. Day 4 Wed, October 16, 2019. Published online October 13, 2019. doi: 10.2118/198033-ms
28. Krishnan M, Chen HY, Ho RM. Switchable structural colors from mesoporous polystyrene films. In: AMER CHEMICAL SOC 1155 16TH ST, NW, WASHINGTON, DC 20036 USA; 2016.
29. Krishnan MR, Rajendran V, Alsharaeh E. Anti-reflective and high-transmittance optical films based on nanoporous silicon dioxide fabricated from templated synthesis. Journal of Non-Crystalline Solids. 2023; 606: 122198. doi: 10.1016/j.jnoncrysol.2023.122198
30. Krishnan MR, Omar H, Almohsin A, et al. An overview on nanosilica–polymer composites as high-performance functional materials in oil fields. Polymer Bulletin. 2023; 81(5): 3883-3933. doi: 10.1007/s00289-023-04934-y
31. Krishnan MR, Li W, Alsharaeh EH. Cross-linked polymer nanocomposite networks coated nano sand light-weight proppants for hydraulic fracturing applications. Characterization and Application of Nanomaterials. 2023; 6(2): 3314. doi: 10.24294/can.v6i2.3314
32. Krishnan MR, Almohsin A, Alsharaeh EH. Syntheses and fabrication of mesoporous styrene-co-methyl methacrylate-graphene composites for oil removal. Diamond and Related Materials. 2022; 130: 109494. doi: 10.1016/j.diamond.2022.109494
33. Krishnan MR, Li W, Alsharaeh EH. Ultra-lightweight Nanosand/Polymer Nanocomposite Materials for Hydraulic Fracturing Operations. SSRN Electronic Journal. Published online 2022. doi: 10.2139/ssrn.4233321
34. Krishnan MR, Michael FM, Almohsin A, et al. Polyacrylamide Hydrogels Coated Super-hydrophilic Sand for Enhanced Water Storage and Extended Release. SSRN Electronic Journal. Published online 2022. doi: 10.2139/ssrn.4232876
35. Krishnan MR, Lu K, Chiu W, et al. Directed Self-Assembly of Star-Block Copolymers by Topographic Nanopatterns through Nucleation and Growth Mechanism. Small. 2018; 14(16). doi: 10.1002/smll.201704005
36. Krishnan MR, Chien YC, Cheng CF, et al. Fabrication of Mesoporous Polystyrene Films with Controlled Porosity and Pore Size by Solvent Annealing for Templated Syntheses. Langmuir. 2017; 33(34): 8428-8435. doi: 10.1021/acs.langmuir.7b02195
37. Krishnan MR, Samitsu S, Fujii Y, et al. Hydrophilic polymer nanofibre networks for rapid removal of aromatic compounds from water. Chem Commun. 2014; 50(66): 9393-9396. doi: 10.1039/c4cc01786b
38. Krishnan MR, Almohsin A, Alsharaeh EH. Thermo-Mechanically Reinforced Mesoporous Styrene-Co-Methyl Methacrylate-Graphene Composites for Produced Water Treatment. Available online: https://papers.ssrn.com/sol3/papers.cfm?abstract_id=4207331 (accessed on 1 March 2024).
39. Krishnan MR, Alsharaeh E. Potential removal of benzene-toluene-xylene toxic vapors by nanoporous poly(styrene-r-methylmethacrylate) copolymer composites. Environmental Nanotechnology, Monitoring & Management. 2023; 20: 100860. doi: 10.1016/j.enmm.2023.100860
40. Krishnan MR, Alsharaeh EH. A Review on Polymer Nanocomposites Based High-Performance Functional Materials. SSRN Electronic Journal. Published online 2022. doi: 10.2139/ssrn.4222854
41. Krishnan MR, Rajendran V. Sulfonated mesoporous polystyrene-1D multiwall carbon nanotube nanocomposite as potential adsorbent for efficient removal of xylene isomers from aqueous solution. Characterization and Application of Nanomaterials. 2023; 6(2): 3516. doi: 10.24294/can.v6i2.3516
42. Lo TY, Krishnan MR, Lu KY, et al. Silicon-containing block copolymers for lithographic applications. Progress in Polymer Science. 2018; 77: 19-68. doi: 10.1016/j.progpolymsci.2017.10.002
43. Samitsu S, Zhang R, Peng X, et al. Flash freezing route to mesoporous polymer nanofibre networks. Nature Communications. 2013; 4(1). doi: 10.1038/ncomms3653
44. Kolay PK, Dhakal B. Geotechnical Properties and Microstructure of Liquid Polymer Amended Fine-Grained Soils. Geotechnical and Geological Engineering. 2019; 38(3): 2479-2491. doi: 10.1007/s10706-019-01163-x
45. Alsharaeh EH, Krishnan MR. Method of making mutlilayer soil with property for extended release water for desert agriculture. US10772265B1, 15 September 2020.
46. Krishnan MR, Omar H, Yazeed Y, et al. Insight into Thermo-Mechanical Enhancement of Polymer Nanocomposites Coated Microsand Proppants for Hydraulic Fracturing. SSRN Electronic Journal. Published online 2022. doi: 10.2139/ssrn.4243574
47. Krishnan MR, Aldawsari Y, Michael FM, et al. 3D-Polystyrene-polymethyl methacrylate/divinyl benzene networks-Epoxy-Graphene nanocomposites dual-coated sand as high strength proppants for hydraulic fracture operations. Journal of Natural Gas Science and Engineering. 2021; 88: 103790. doi: 10.1016/j.jngse.2020.103790

48. Krishnan MR, Aldawsari Y, Michael FM, et al. Mechanically reinforced polystyrene-polymethyl methacrylate copolymer-graphene and Epoxy-Graphene composites dual-coated sand proppants for hydraulic fracture operations. Journal of Petroleum Science and Engineering. 2021; 196: 107744. doi: 10.1016/j.petrol.2020.107744
49. Michael FM, Krishnan MR, Li W, et al. A review on polymer-nanofiller composites in developing coated sand proppants for hydraulic fracturing. Journal of Natural Gas Science and Engineering. 2020; 83: 103553. doi: 10.1016/j.jngse.2020.103553
50. Almohsin A, Krishnan MR, Alsharaeh E, et al. Preparation and Properties Investigation on Sand-Polyacrylamide Composites with Engineered Interfaces for Water Shutoff Applications. Day 2 Mon, February 20, 2023. Published online March 7, 2023. doi: 10.2118/213481-ms
51. Almohsin A, Alsharaeh E, Krishnan MR. Polymer-sand nanocomposite lost circulation material. US11828116B2, 28 November 2023.
52. Almohsin A, Alsharaeh E, Krishnan MR, et al. Coated nanosand as relative permeability modifier. US11827852B2, 28 November 2023.
53. Almohsin A, Alsharaeh E, Michael FM, et al. Polymer-Nanofiller Hydrogels. US11802232B2, 31 October 2023.
54. Krishnan MR, Almohsin A, Alsharaeh EH. Mechanically robust and thermally enhanced sand-polyacrylamide-2D nanofiller composite hydrogels for water shutoff applications. Journal of Applied Polymer Science. 2023; 141(7). doi: 10.1002/app.54953
55. Li W, Alsharaeh E, Krishnan MR. Methods for making proppant coatings. US11459503B2, 4 October 2022.
56. Li W, Alsharaeh E, Krishnan MR. Proppant coatings and methods of making. US11851614B2, 26 December 2023.
57. Krishnan MR, Alsharaeh EH. Facile fabrication of thermo-mechanically reinforced polystyrene-graphene nanocomposite aerogel for produced water treatment. Journal of Porous Materials. Published online April 12, 2024. doi: 10.1007/s10934-024-01602-y
58. Krishnan MR, Omar H, Almohsin A, et al. An overview on nanosilica–polymer composites as high-performance functional materials in oil fields. Polymer Bulletin. 2023; 81(5): 3883-3933. doi: 10.1007/s00289-023-04934-y
59. Krishnan MR, Alsharaeh EH. High-performance functional materials based on polymer nanocomposites—A review. Journal of Polymer Science and Engineering. 2023; 6(1): 3292. doi: 10.24294/jpse.v6i1.3292
60. Krishnan MR, Alsharaeh EH. Polymer gel amended sandy soil with enhanced water storage and extended release capabilities for sustainable desert agriculture. Journal of Polymer Science and Engineering. 2023; 6(1): 2892. doi: 10.24294/jpse.v6i1.2892
61. Krishnan MR, Aldawsari YF, Alsharaeh EH. 3D-poly (styrene-methyl methacrylate)/divinyl benzene-2D-nanosheet composite networks for organic solvents and crude oil spill cleanup. Polymer Bulletin. 2021; 79(6): 3779-3802. doi: 10.1007/s00289-021-03565-5
62. Krishnan MR, Aldawsari YF, Alsharaeh EH. Three-dimensionally cross-linked styrene-methyl methacrylate-divinyl benzene terpolymer networks for organic solvents and crude oil absorption. Journal of Applied Polymer Science. 2020; 138(9). doi: 10.1002/app.49942
63. O'rourke TD, Druschel SJ, Netravali AN. Shear strength characteristics of sand-polymer interfaces. Journal of Geotechnical Engineering. 1990; 116 (3): 451-469. doi: 10.1061/(ASCE)0733-9410(1990)116:3(451)